John Barnard
Steven Lund
USPAS
June 13-24, 2011
Melville, NY

An application of intense beams

1. Heavy-ion fusion
    A. Requirements
    B. Targets for ICF
    C. Accelerator
    D. Drift compression
    E. Final focus
    F. Experiments

Inertial fusion energy (IFE) power plants of the future will consist of four parts

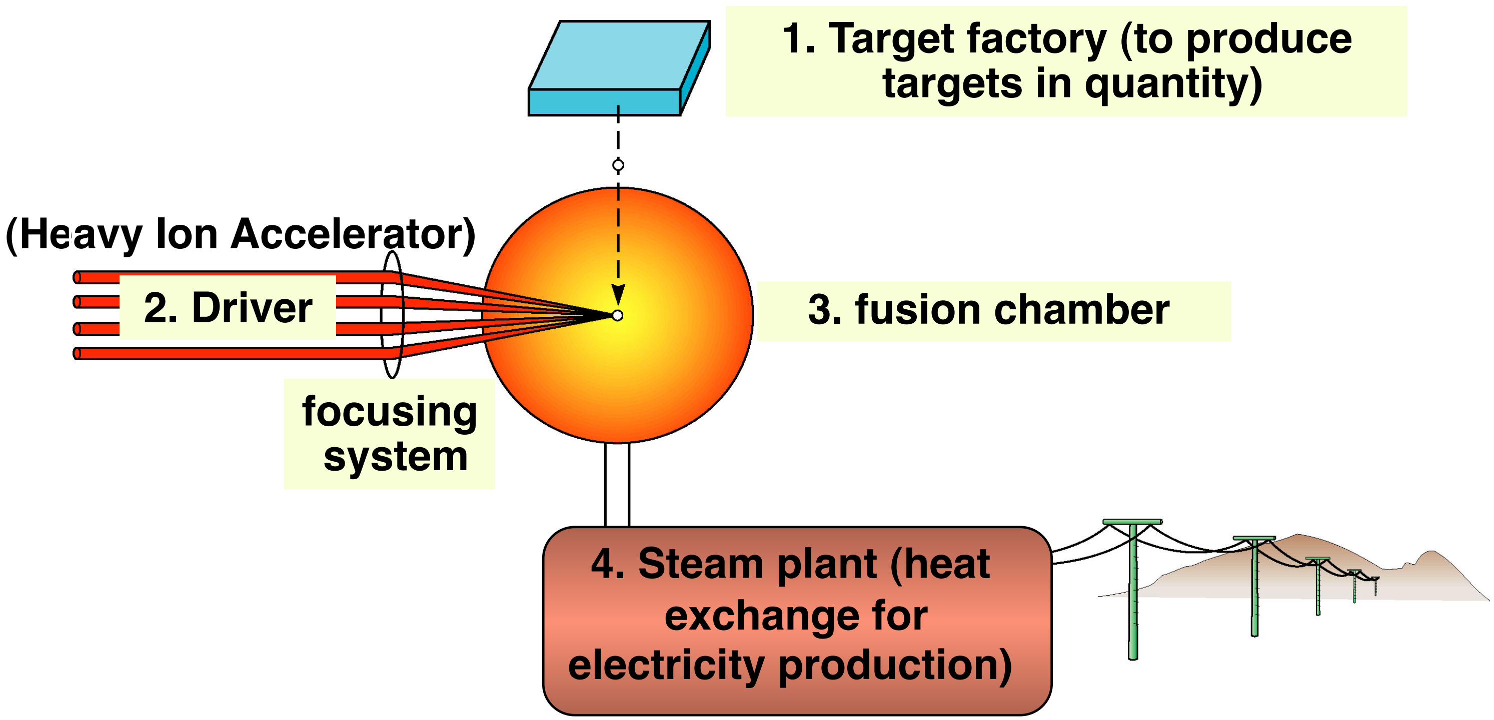

A power plant driver would fire about five targets per second to produce as much electricity as today's 1000 Megawatt power plant

Heavy Ion Fusion provides an attractive approach to long term energy production

Fusion offers an inexaustible, long term solution to the problem of future energy supplies free from long-lived radioactive by-products and greenhouse CO_2.

Inertial Confinement Fusion (ICF) uses laser or particle beams to implode a target, raising the temperature and density of the fuel, creating the conditions necessary for the following reaction:

$$D + T \rightarrow n\ (14.06\ \mathrm{MeV}) + He^4\ (3.52\ \mathrm{MeV})\ .$$

Heavy ion accelerators are a strong candidate for inertial fusion *energy production* (IFE) because of:

- High efficiency
- High repetition rate
- Survivability of final lens
- Favorable target illumination geometry

National Ignition Facility (NIF) at LLNL plays a critical role in addressing IFE feasibility

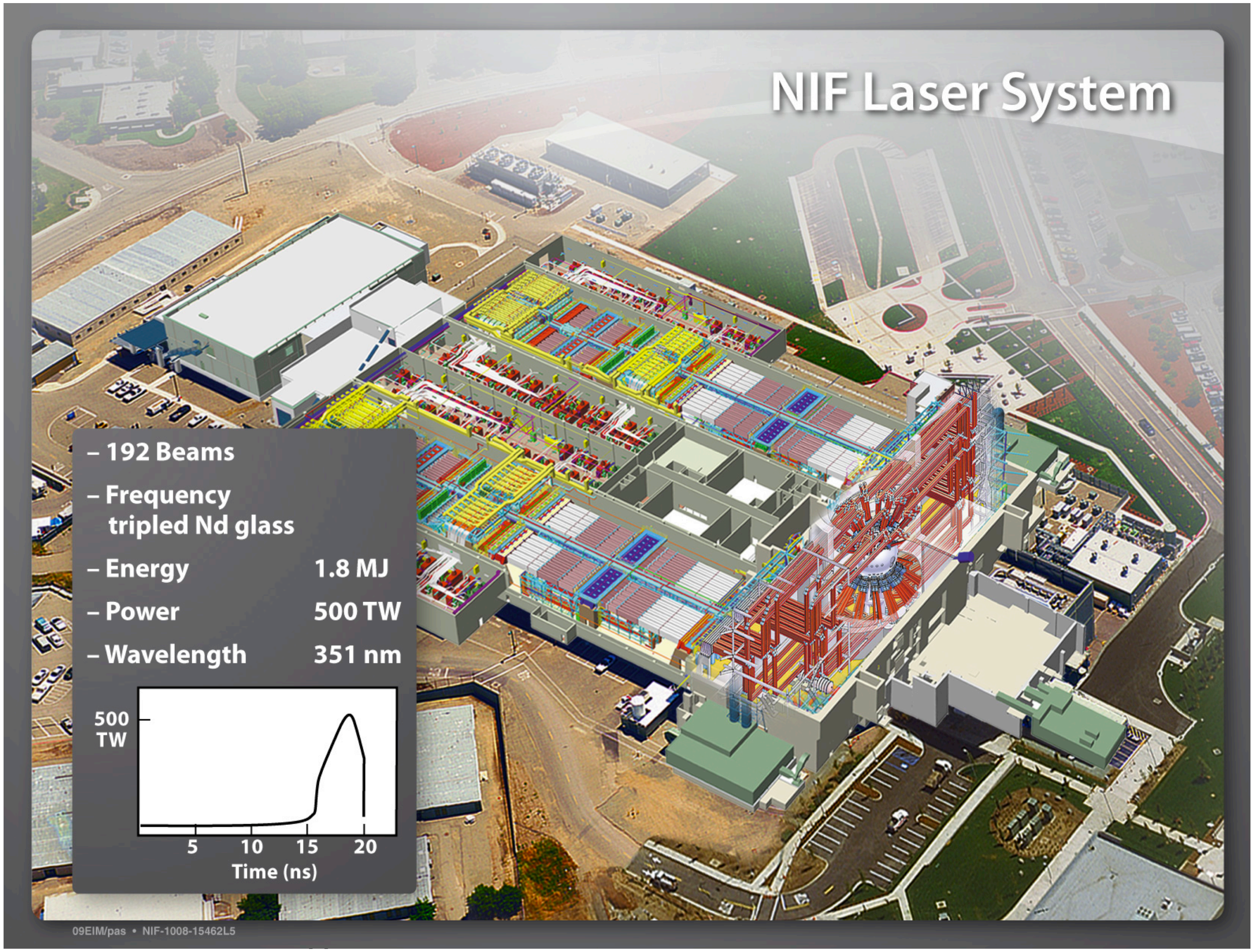




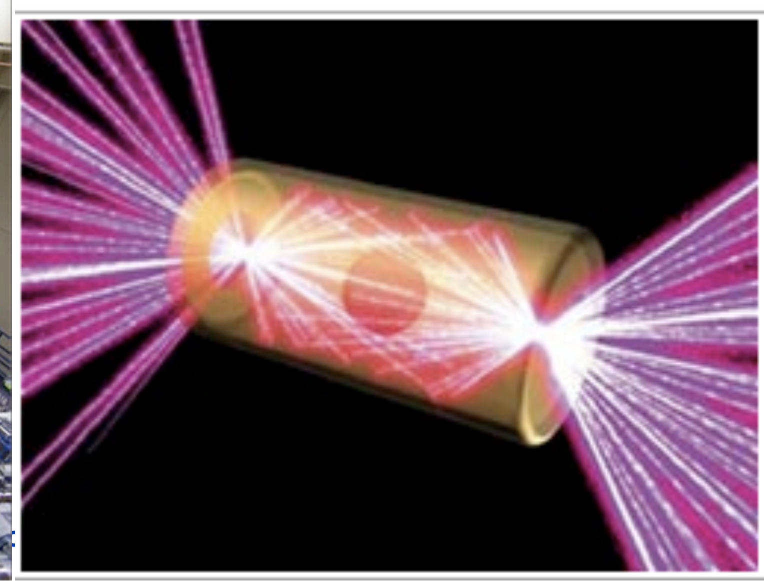

The two principal approaches to ICF are direct drive and indirect drive

Two types of targets:

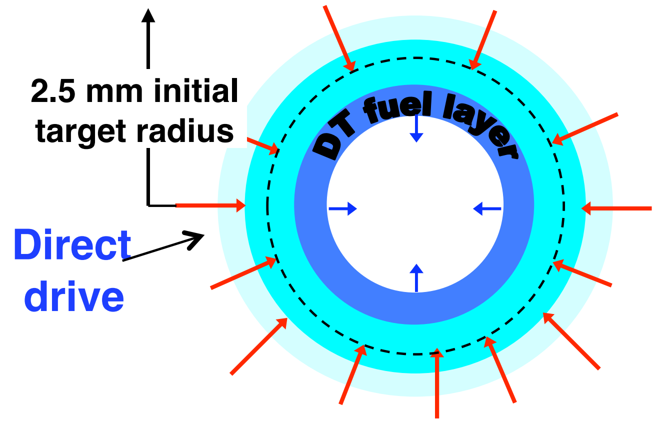

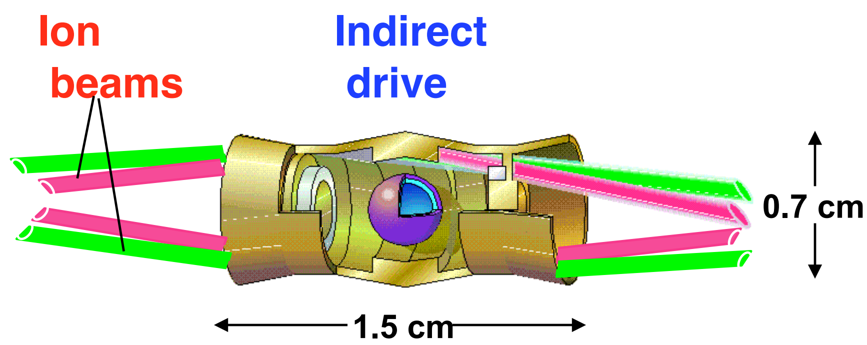

Direct drive advantages:

Higher coupling efficiency with potential for higher gain

Indirect drive advantages:

Relaxed beam uniformity (reduced hydro instability)

SIgnificant commonality for lasers and ion beams

Significant simplification of chamber geometry

“Fast ignition” is an alternative to “hot spot ignition”

- Capsule is compressed on low adiabat
- Second “igniter” pulse starts ignition process

Compression pulse:
Pulse energy ~ 200 kJ – 1 MJ
Pulse duration ~ 10 ns
Spot radius ~ 2 mm

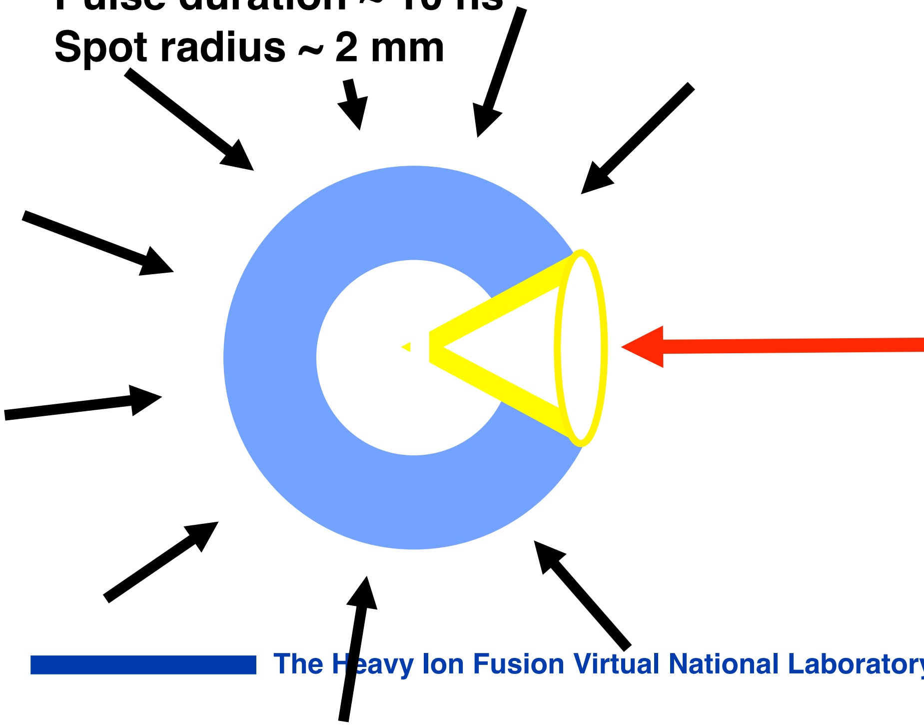

Igniter pulse: (creates electron or ion beam)
Pulse energy ~ 200 kJ – 1 MJ
Pulse duration ~ 20 ps
Spot radius ~ 20 μ

The X-Target-Mark2: XMK2

20 GeV Rubidium beams (0.5+0.5+2.0 = 3.0 MJ)
Yield = 1.2 GJ

1st, 2nd, and ignition beams are many beams with overlapping spots modeled as annuli

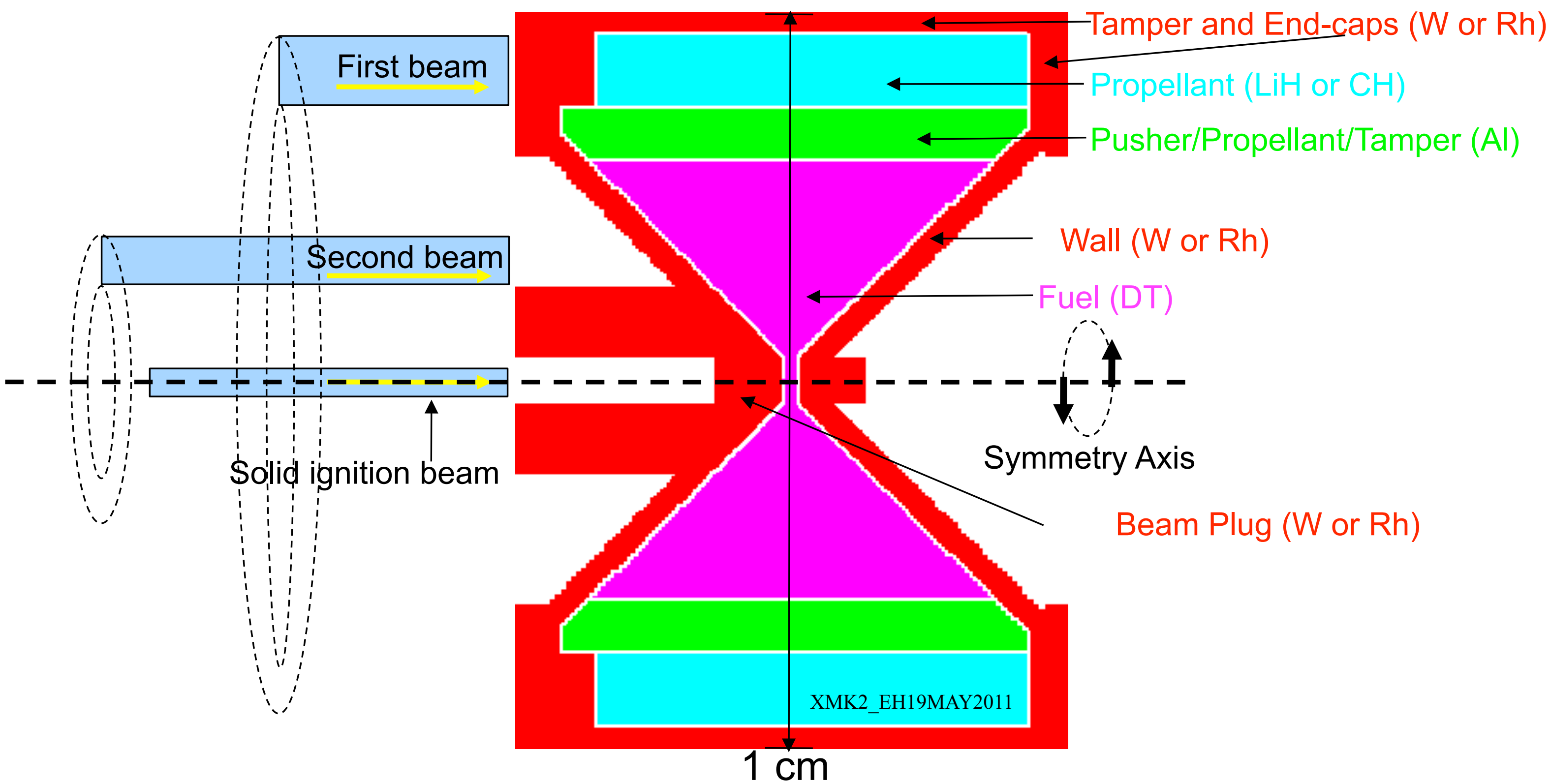

A "distributed radiator" target produces high gain in radiation/hydrodynamic simulations

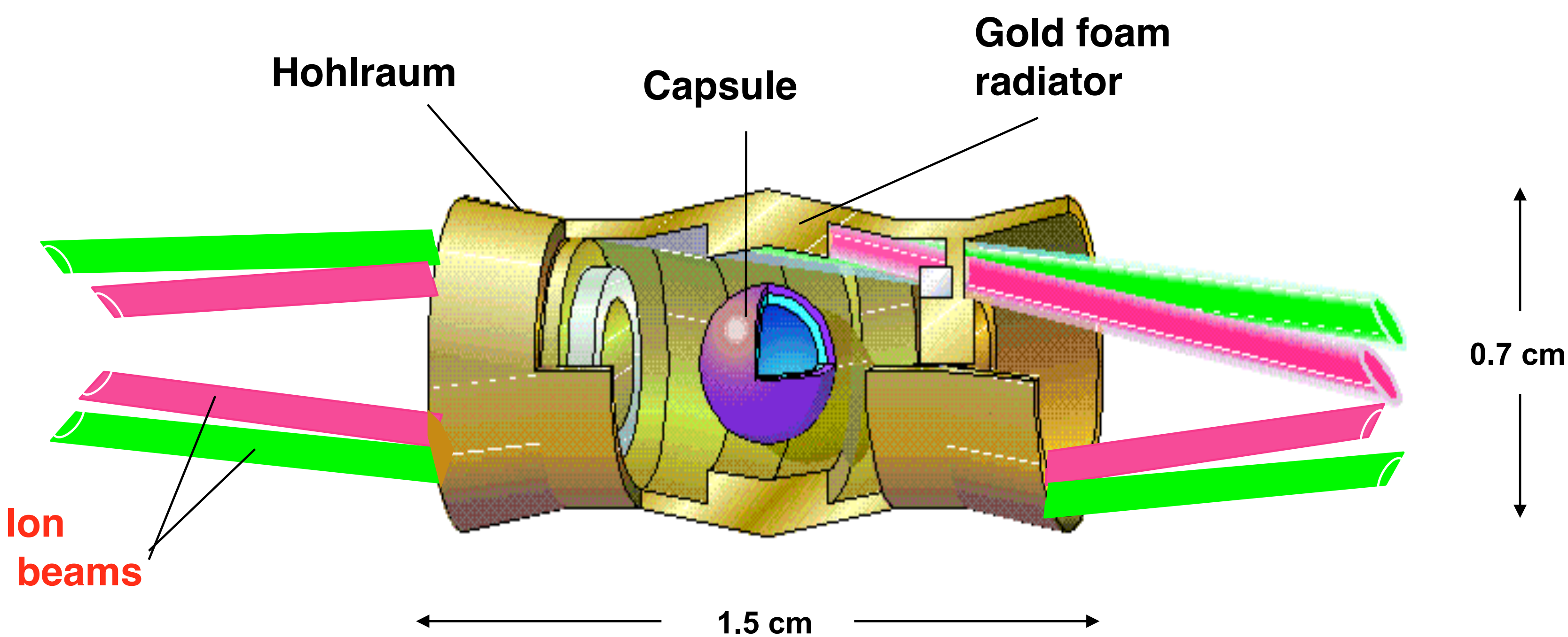

Focusability at the target is key scientific issue

Conditions of beam at target are set by hohlraum and implosion physics

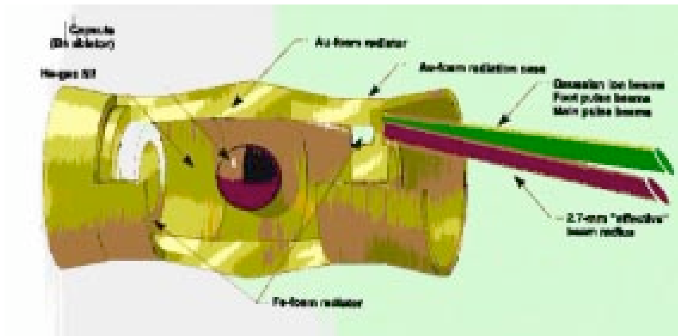

Energy in pulse: ~ 3 to 6 MJ

Duration of main pulse: ~ 8 to 10 ns

Duration of foot pulse: ~ 30 ns

Spot radius: ~ 1.5 to 3 mm

Transverse and longitudinal compression are required to meet target specifications.

y
z

Length of beam just outside of injector ~25-50 m

At target ~ 0.5 - 1 m

y
x

Radius of beam at source ~ 1-3 cm

At target ~ 1.5-3 mm

Compression factors of 10 to 50 in both longitudinal and transverse directions are required.

Overlapping Gaussian, elliptical beams are focused at the end of the target

Each beam is an ellipse

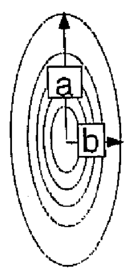

a = 4.15 mm
b = 1.8 mm
effective r=2.7 mm
95% of charge inside

8 beams overlap in the foot pulse

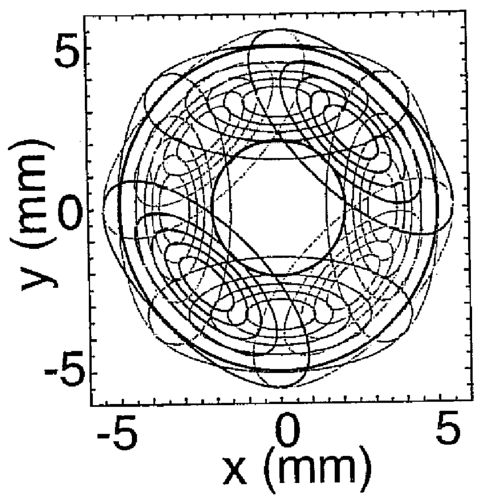

Sum of 8 foot pulse beams

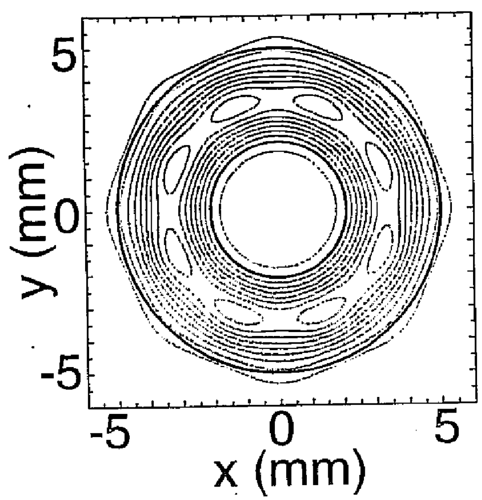

Azimuthal asymmetry:
foot pulse: -1.6% in m=8
main pulse: 0.06% in m=16

Callahan 8/97

Ion current profile and radiation temperature

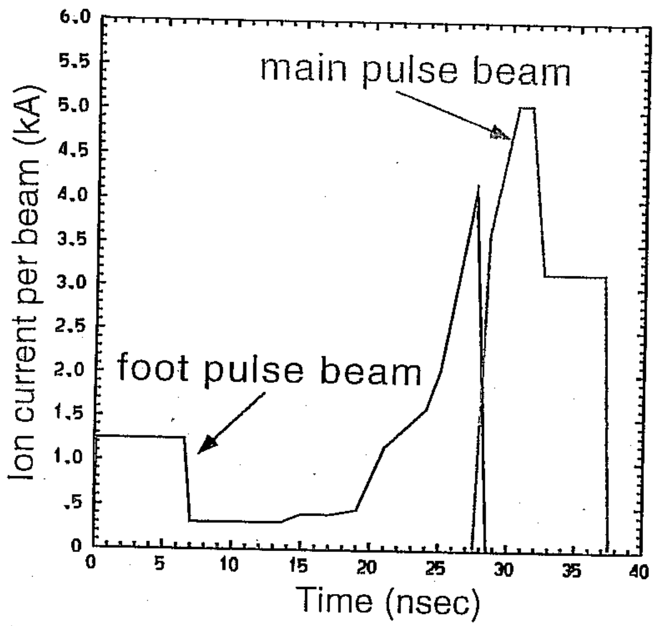

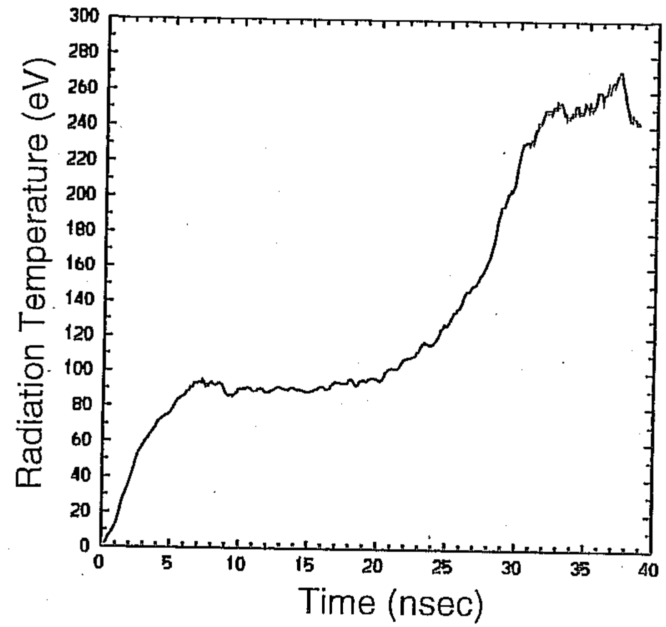

Current assumes 16 beams in foot pulse
32 beams in main pulse

Callahan 11/97

Why Heavy Ions?

<u>Target requires</u>:

3.5 - 6 MJ in ~ 10 ns $\Rightarrow$ ~ 500 TW

Range ~ 0.02 - .2 g/cm^2

Range requirement $\downarrow$

Higher mass $\Leftrightarrow$ higher kinetic energy

Power Requirement $\downarrow$

Current $\propto \frac{1}{\text{kinetic energy}}$

$\boxed{\text{Higher mass requires lower current (easier to focus).}}$

6

Heavier Ions ⇒ Higher Kinetic Energy

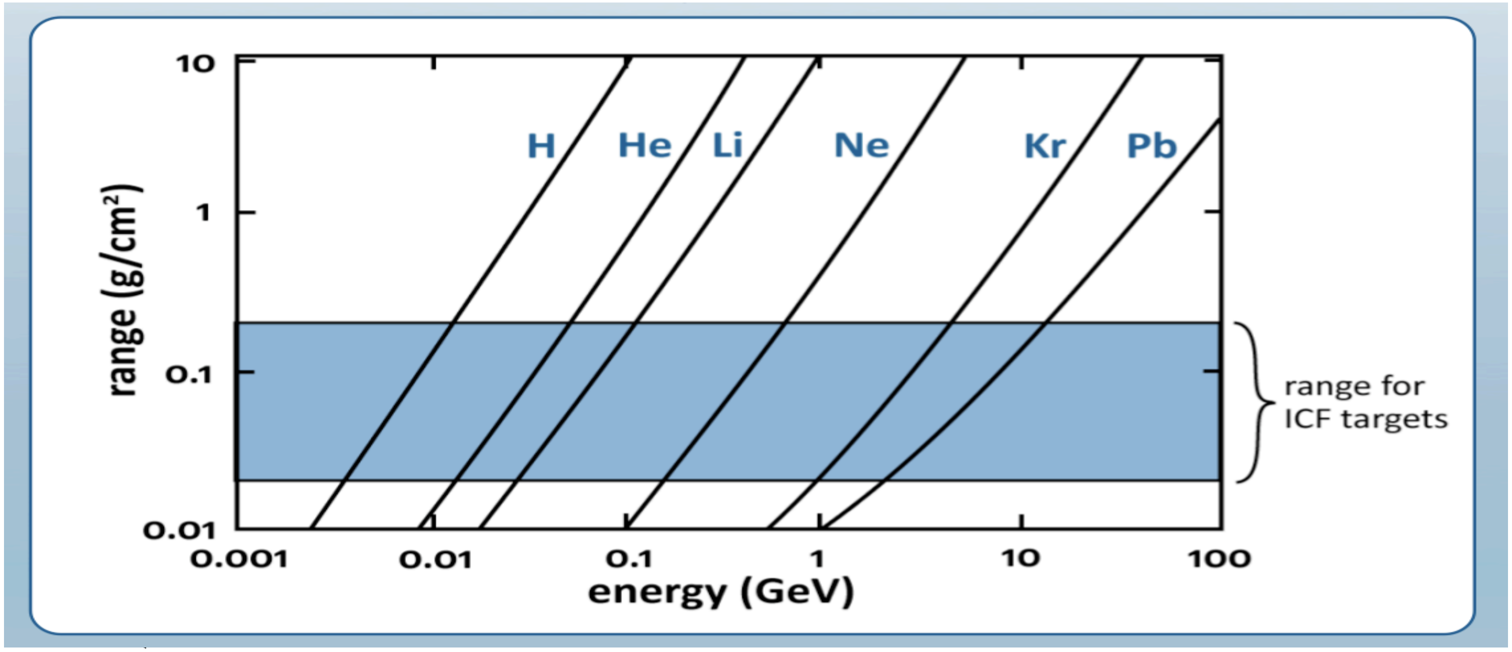

Targets require high power (kinetic energy x current).

- Light Ion Fusion requires high-current, unconventional accelerators (Sandia 1970s).
- Heavy Ion Fusion requires lower currents enabling the use of more conventional high energy accelerators (Maschke ~ 1974).

There are two principle methods of acceleration

1. r.f. acceleration

(Approach in Europe and Japan)

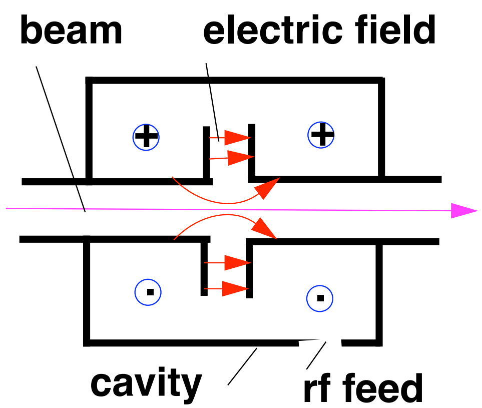

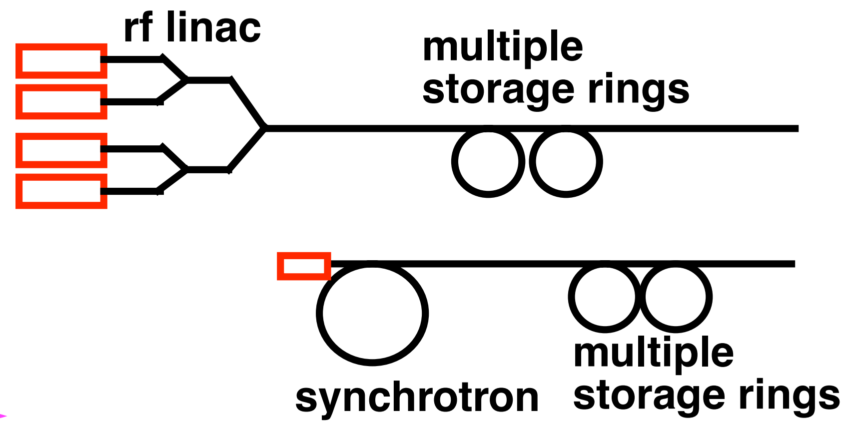

2. Induction acceleration

(U.S. approach)

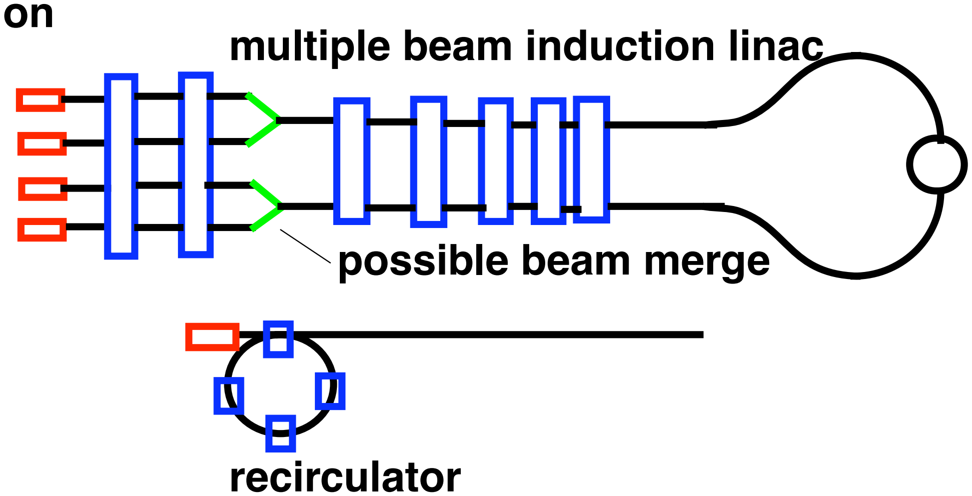

Induction acceleration for HIF consists of several subsystems and a variety of beam manipulations

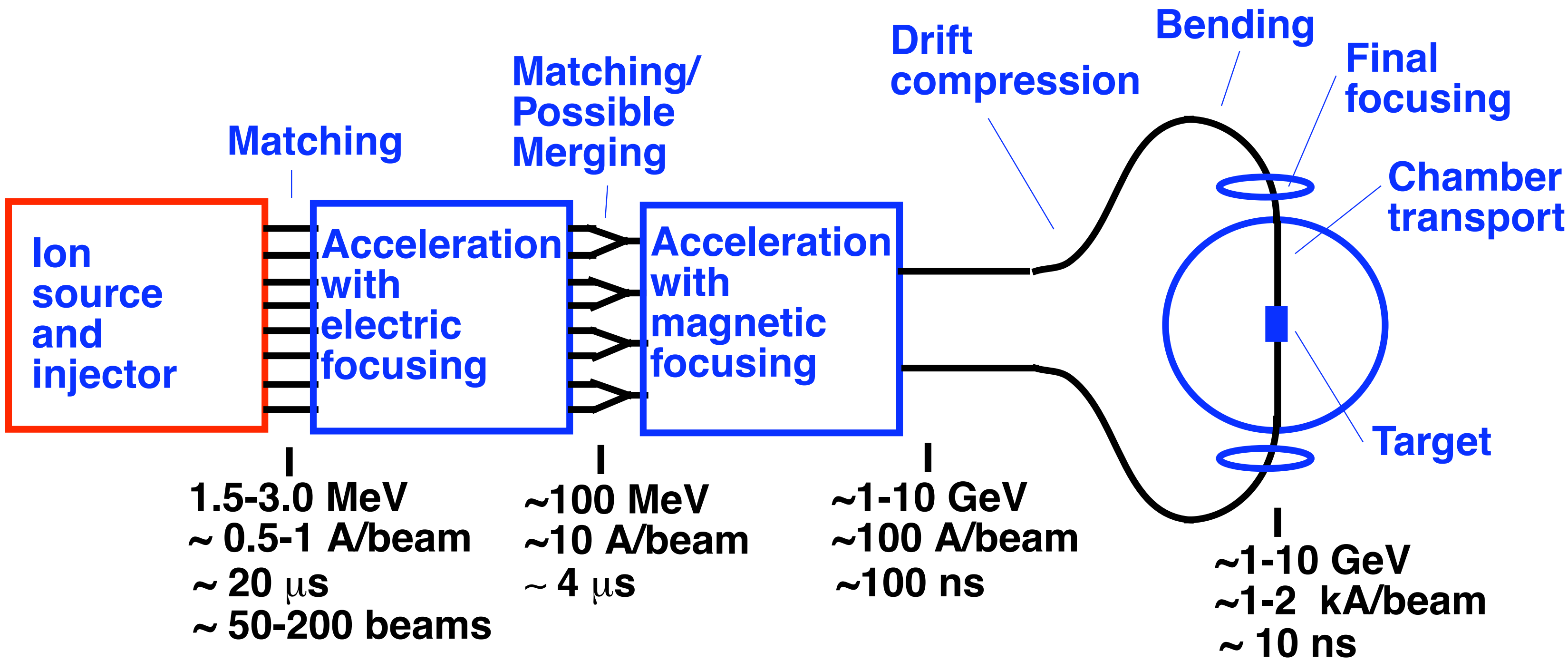

A “Robust Point Design” design study established a baseline for a multibeam quadrupolar linac HIF driver

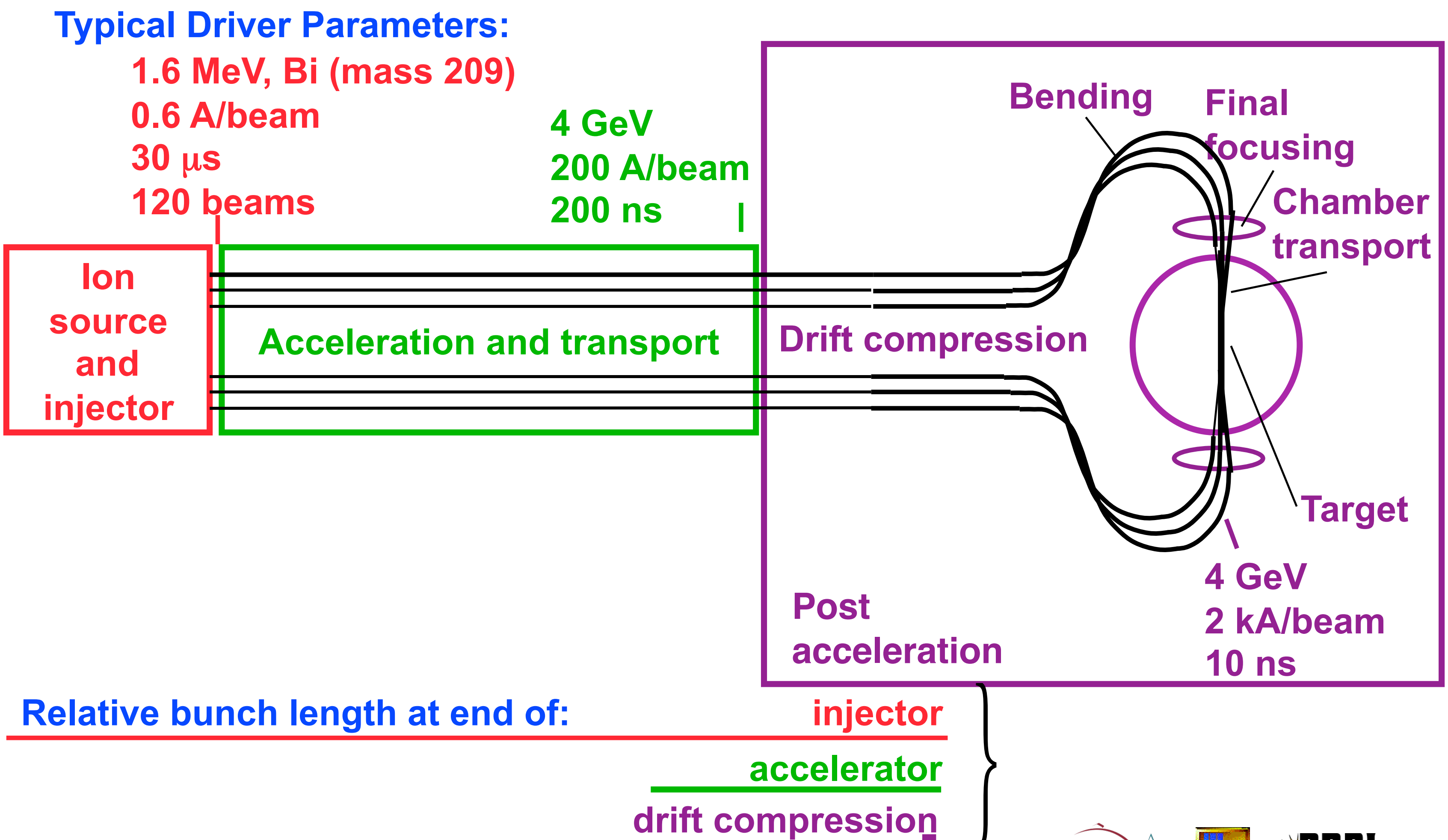

Summary of Current Limits From Different Focusing Methods

Einzel Lens

$$Q_{max} \cong \frac{3\pi^2}{8}\left(\frac{q\phi_0}{m v_0^2}\right)^2\left(\frac{r_b}{L}\right)^2$$

Solenoids

$$Q_{max} = \left(\frac{\omega_c r_b}{2\gamma\beta c}\right)^2$$

Quadrupole Focusing

$$Q_{max} \cong \frac{\eta\Phi_0}{2\pi}\left(\frac{\sin\frac{\eta\pi}{2}}{\frac{\eta\pi}{2}}\right)\left[\begin{array}{l} \frac{B r_b}{[B\rho]}\left[\frac{r_b}{r_p}\right] \quad \text{Magnetic} \\ \frac{2qV_q}{\gamma m v_z^2}\left[\frac{r_b^2}{r_p^2}\right] \quad \text{Electric} \end{array}\right.$$

For Non-Relativistic Beams

$$\lambda_{max} \propto \frac{\phi_0^2}{V} \qquad \lambda_{max} \propto \frac{q}{m} B^2 r_p^2 \qquad \lambda_{max} \propto \begin{cases} B_1 V^{1/2} r_p \\ V_q \end{cases}$$

Note:
ϕ_0 = Voltage between Einzel lenses
V_q = Voltage on a quad relative to ground
V = particle energy$/q$

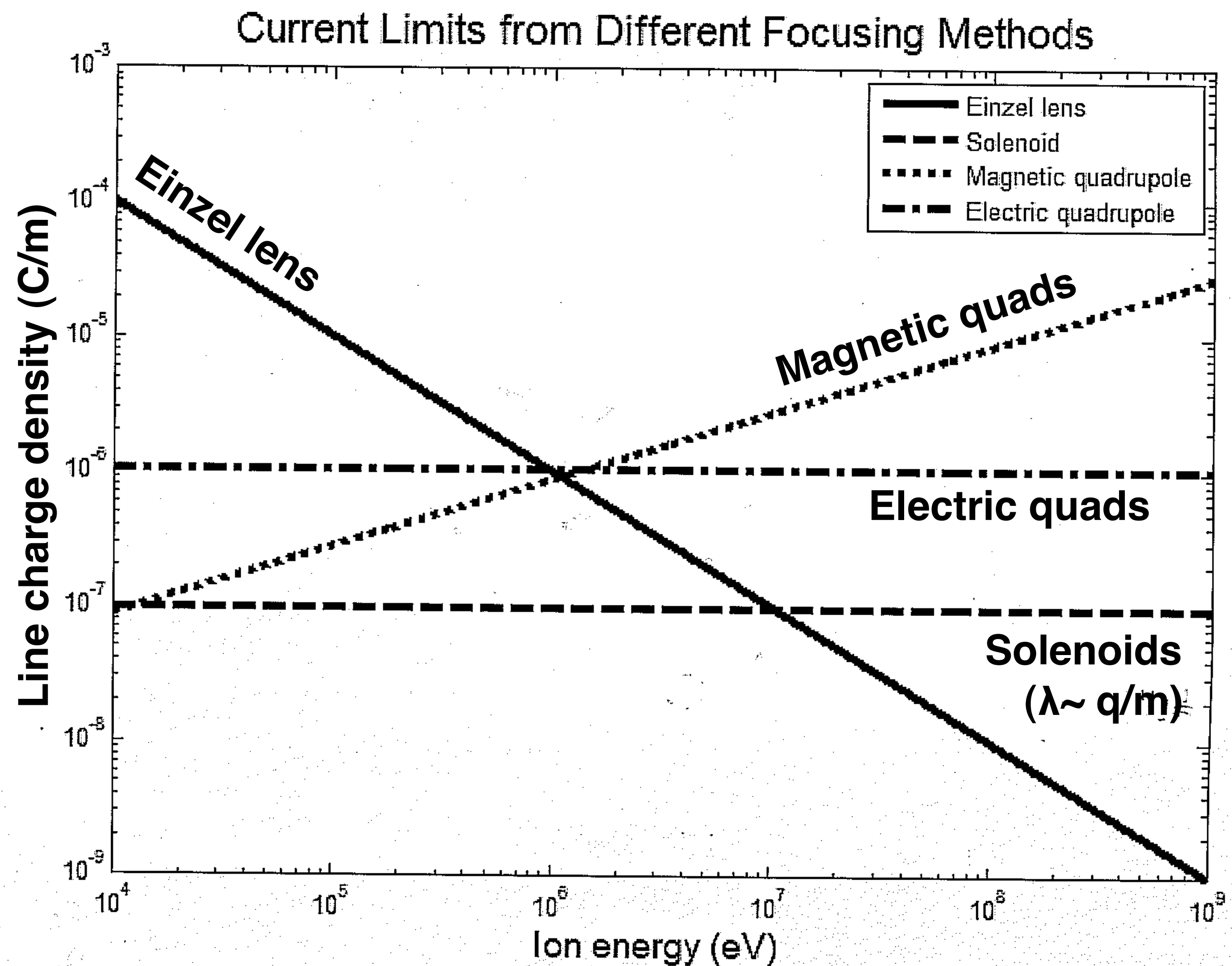

Current Limits from Different Focusing Methods
Line charge density (C/m)
Ion energy (eV)
10^-3
10^-4
10^-5
10^-6
10^-7
10^-8
10^-9
10^4
10^5
10^6
10^7
10^8
10^9
Einzel lens
Solenoid
Magnetic quadrupole
Electric quadrupole
Einzel lens
Magnetic quads
Electric quads
Solenoids
(λ~ q/m)

Major components of induction linac

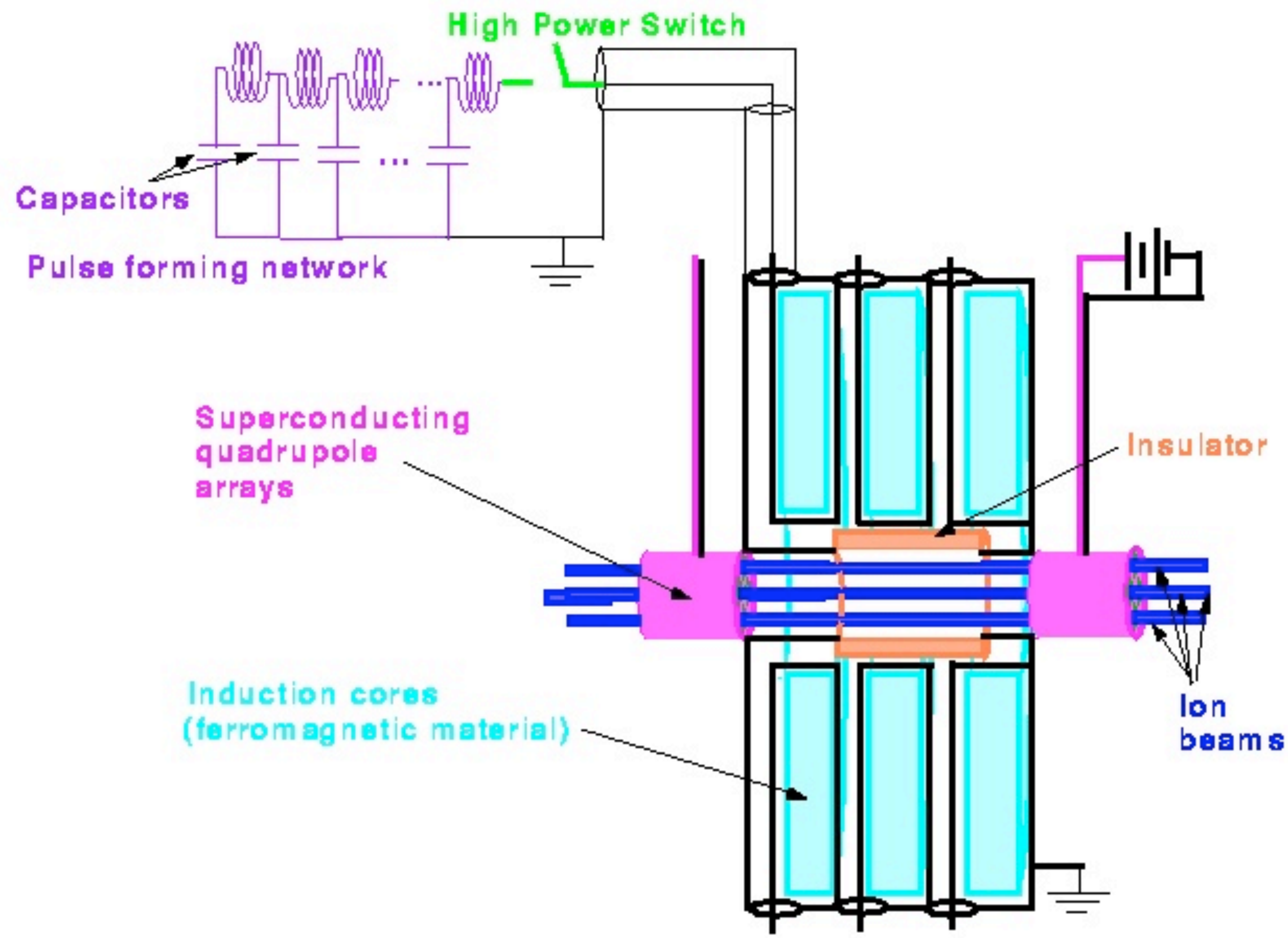

An Induction Core

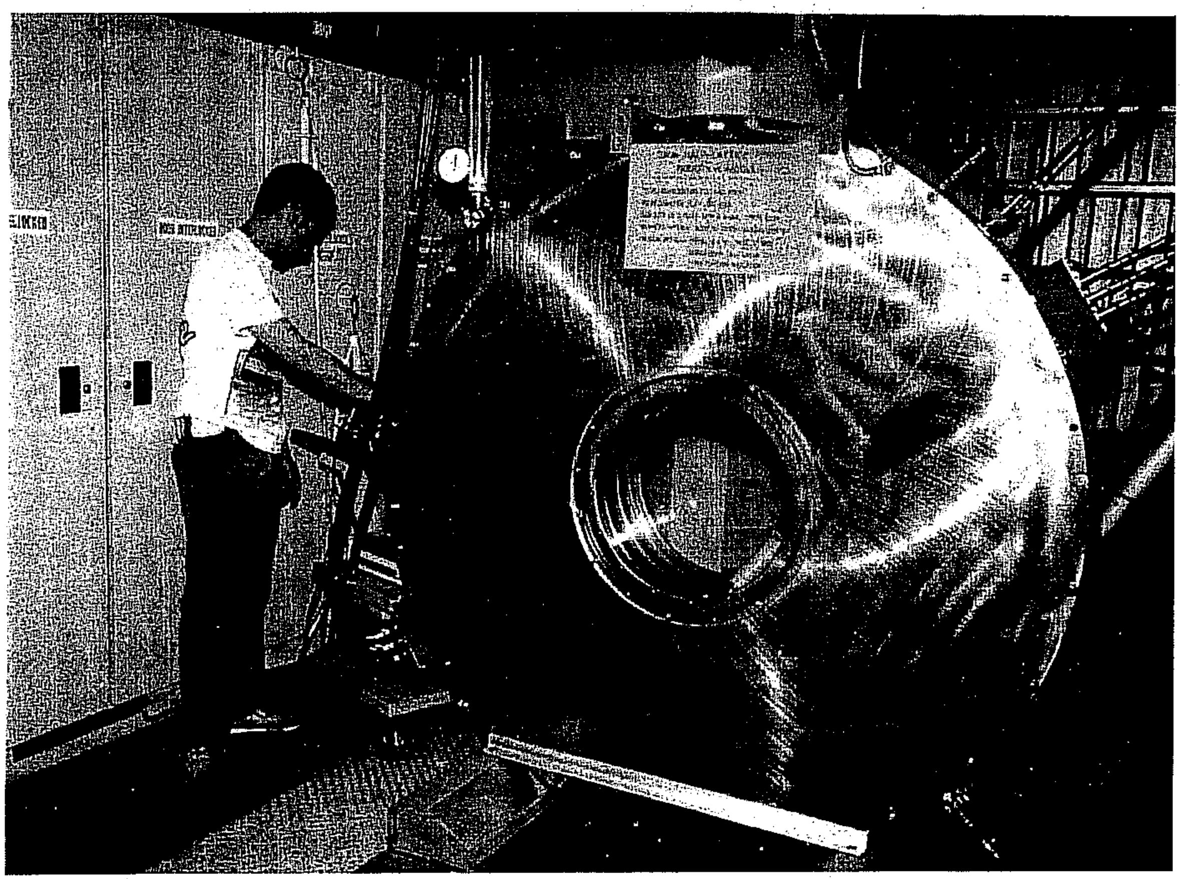

16

An array of small beamlets increases the total beam current through the core

From class:

$$\frac{Q}{a} = \left(\frac{\sigma_0^2}{4L^2}\right) a$$

$$\sigma_0 \cong \frac{\eta L^2 B'}{(B\rho)}$$

$$Q \simeq \frac{\eta B' a}{(B\rho)} \frac{a}{4}$$

$$I \sim \beta^3 Q \sim a^2 B \beta^2 / r_p$$

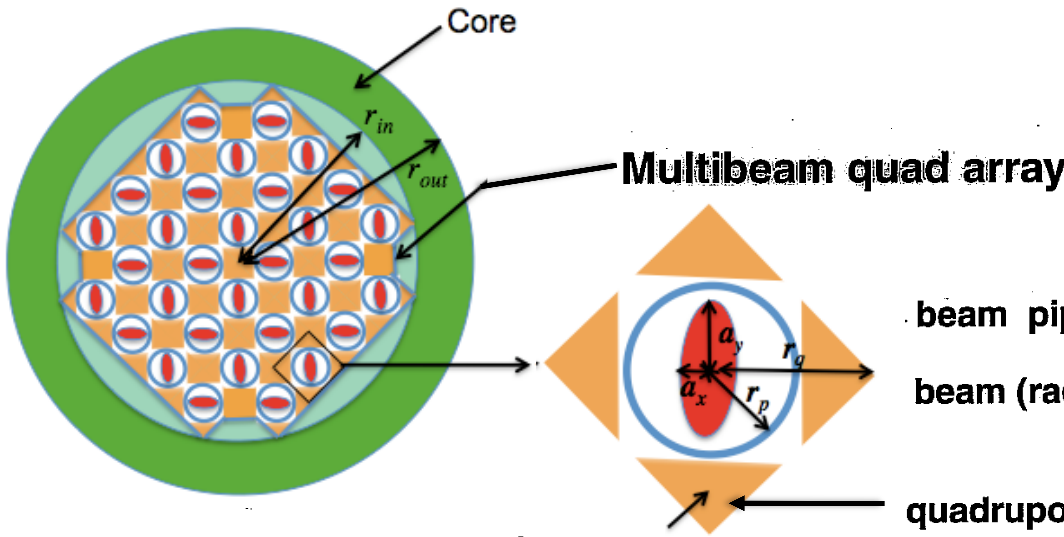

Current per beam = $I_b \sim a^2 B \beta^2 / r_p$

$r_p \sim a$ (until misalignments require minimum size--better: $r_p = c_1 a + c_2$)

so $I_b \sim a$; N_b = number of beams in array $\sim R^2_{core} / a^2$

Total current through core = $I_{tot} = N_b I_b \sim R^2_{core} / a$ (until misalignments dominate scaling)

A Typical driver has about 2000 individual modules

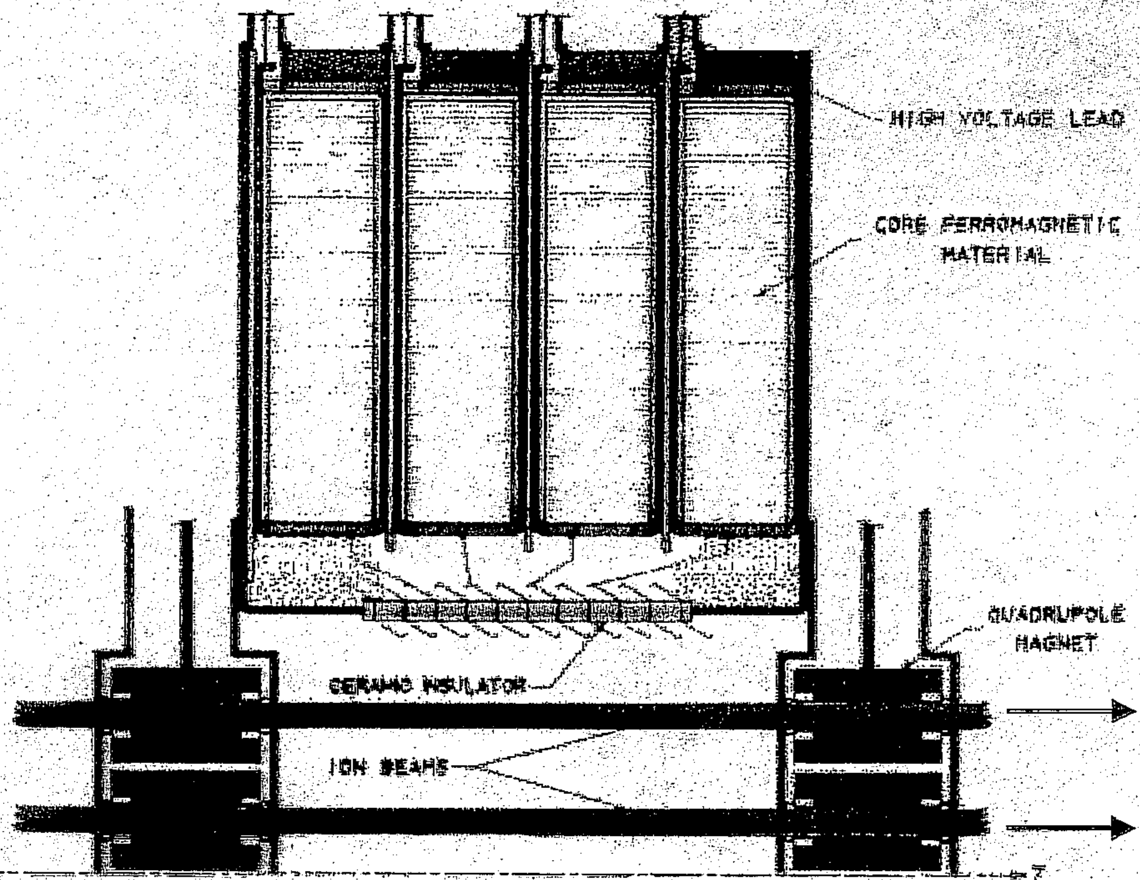

61

In an induction linac, certain limits constrain design

Phase advance per lattice period $\sigma_0 < \sim 85^o$ (to avoid envelope/lattice instabilities and emittance growth)

Space charge is limited by external focusing $K < (\sigma_0 a/2L)^2$ where K is the perveance (proportional to line charge density over beam Voltage), a is the average beam radius and L is the half-lattice period.

Velocity tilt $\Delta v/v <\sim$ 0.3 for electrostatic quads (larger for magnetic quads) to avoid mismatches at head and tail of beam, and to ensure tail radius within pipe and head σ_0 within limit)

Volt-seconds per meter $(dV/ds)\ l/v_0 <\sim$ 1.5-2.0 V-s/m (for "reasonable" core sizes)

Voltage gradient $dV/ds <\sim$ 1-2 MV/m (to avoid breakdown in gaps)

Sources of non-linearity and mismatch are well defined

Sources of non-linearities

- External focusing magnets
- Space-charge
- Multiple-beam effects

Sources of mismatch

- Accelerator imperfections
  - Quad strength and placement errors
  - Acceleration waveform errors
  - Bend strength errors
- Velocity tilt

Simulations give reliable and definitive tolerances on each source

Several potential instabilities have been investigated in HIF drivers

Temperature anisotropy instability

After acceleration $T_{||} << T_{\perp}$, internal beam modes are unstable; saturation occurs when $T_{||} \sim T_{\perp}/3$

Longitudinal resistive instability

Module impedance interacts with beam, amplifying space-charge waves that are backward propagating in beam frame

Beam break-up (BBU) instability

High frequency waves in induction module cavities interact transversely with beam

Beam-plasma instability

Beam interacts with residual gas in target chamber

All of these instabilities have known analytic linear growth rates, which constrain the accelerator design (to ensure minimal growth or benign saturation).

One option for final drift compression is to use a current pulse that is flat with parabolic ends (modeled using the HERMES code)

15 ns final pulse duration

The initial tilt on the beam is about 4% (compare to ~30% at the beginning of the accelerator)

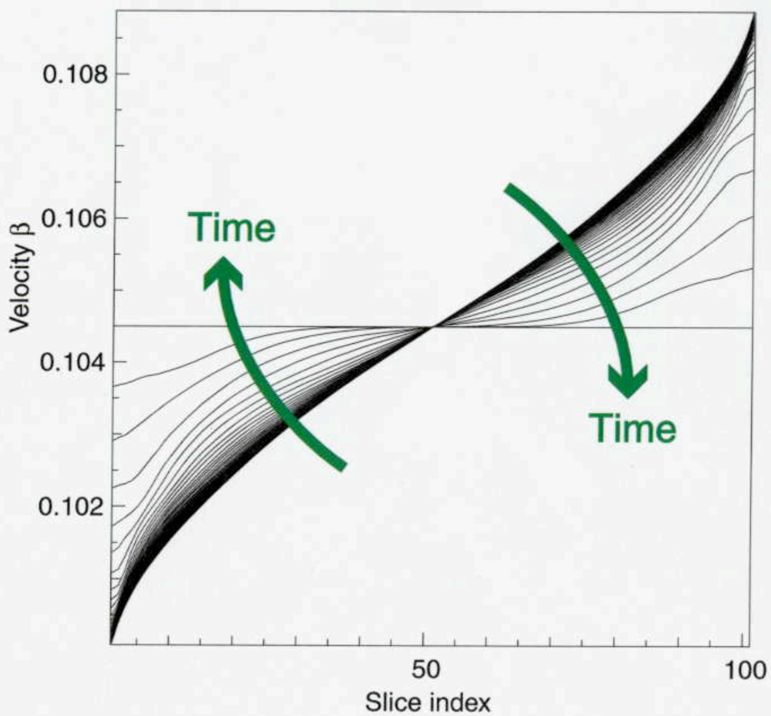

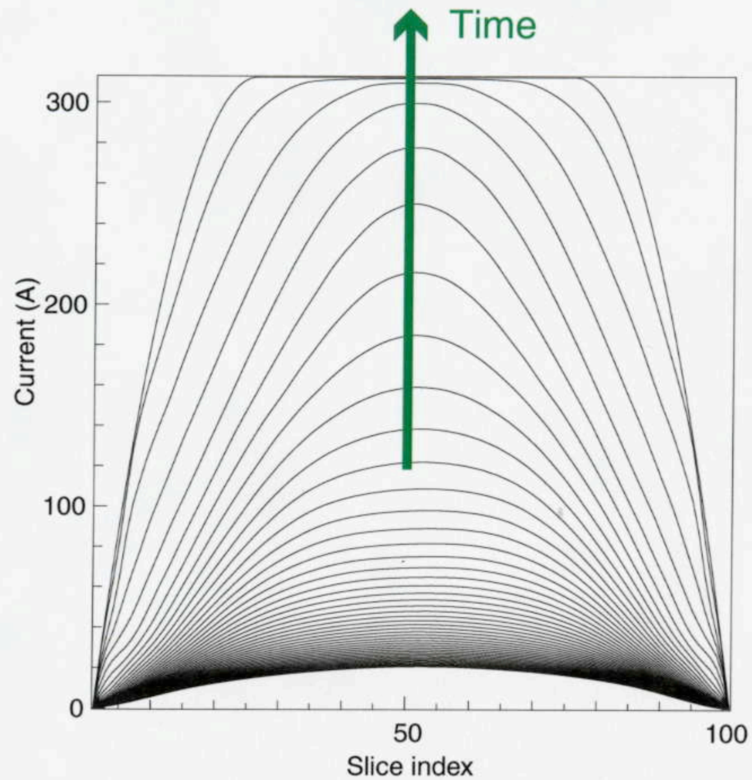

Although the final beam profile is flat, it is parabolic for most of the drift compression

Drift compression section is designed by running code first backwards from target, then forwards after rematching

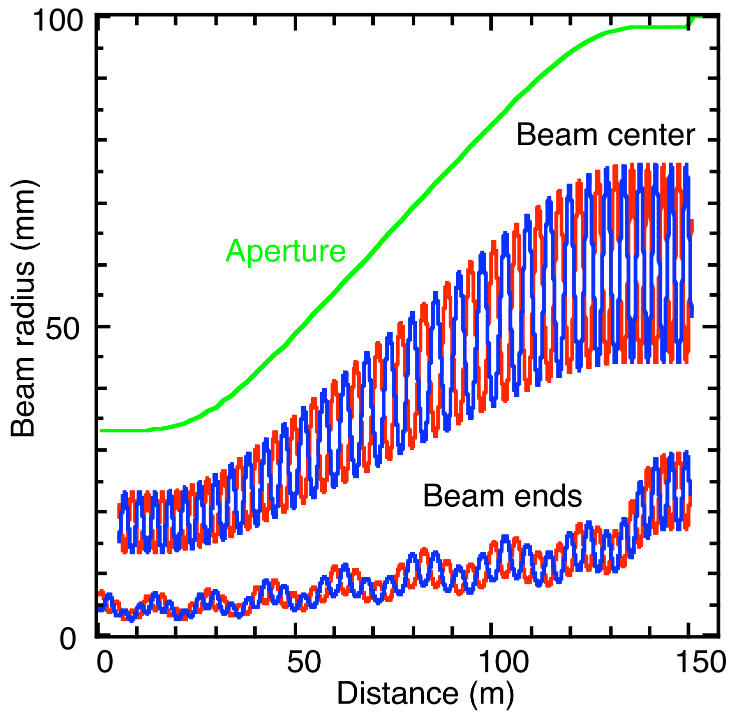

Begin with a desired 20ns, constant -energy pulse at end of compression, track backwards, design lattice for central slice; beam end becomes mismatched early on

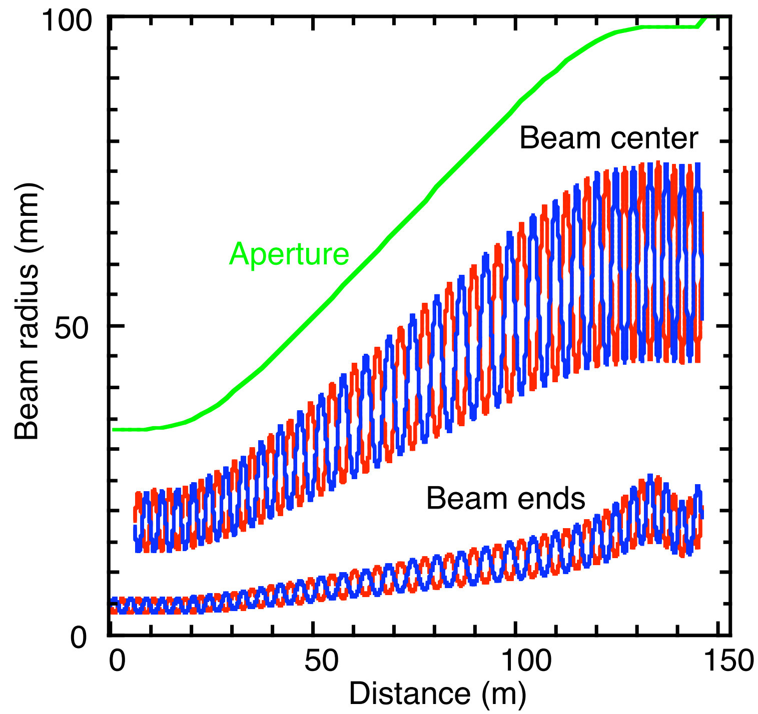

"Rematch" at entrance to compression section, by adjusting a,a',b,b'; then track forward

Heavy ion fusion chamber designs envision using neutronically thick liquid walls to protect solid wall

HYLIFE II chamber concept:

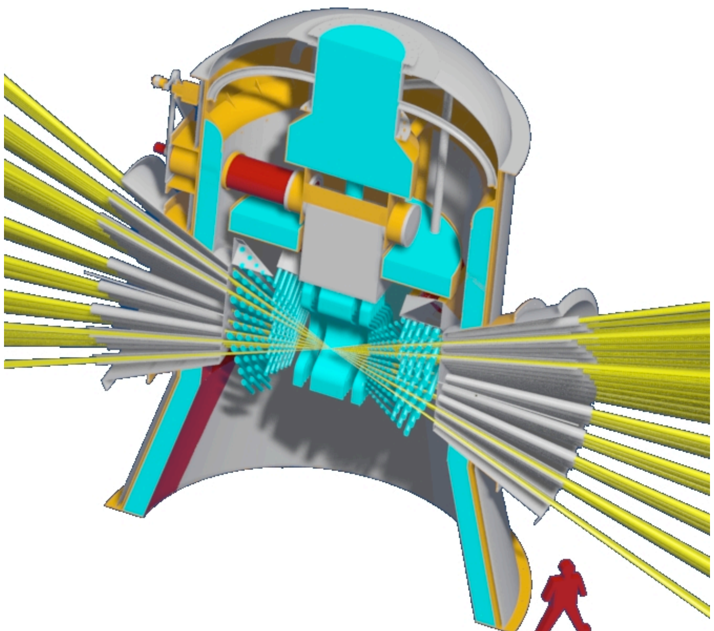

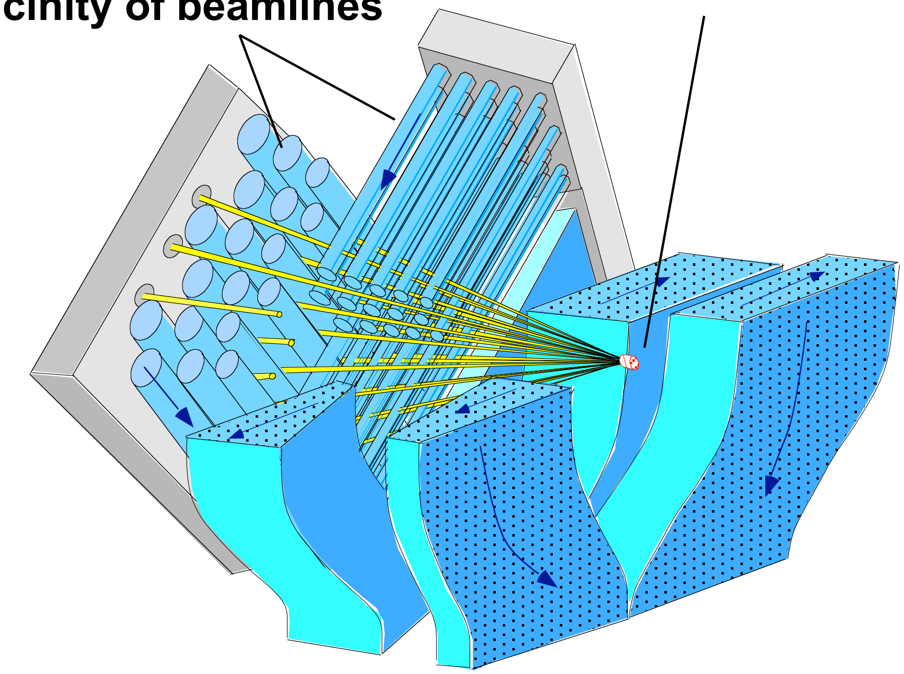

Ion beams shown in gold
FLiBe (a liquid salt) shown in turquoise

The HYLIFE-II Ion beam-driven power plant is shown with a two-end target, illustrated from two sides and a linear heavy-ion induction driver

The liquid wall protection including beam ports is provided by pumping molten salt (Flibe) through the chamber

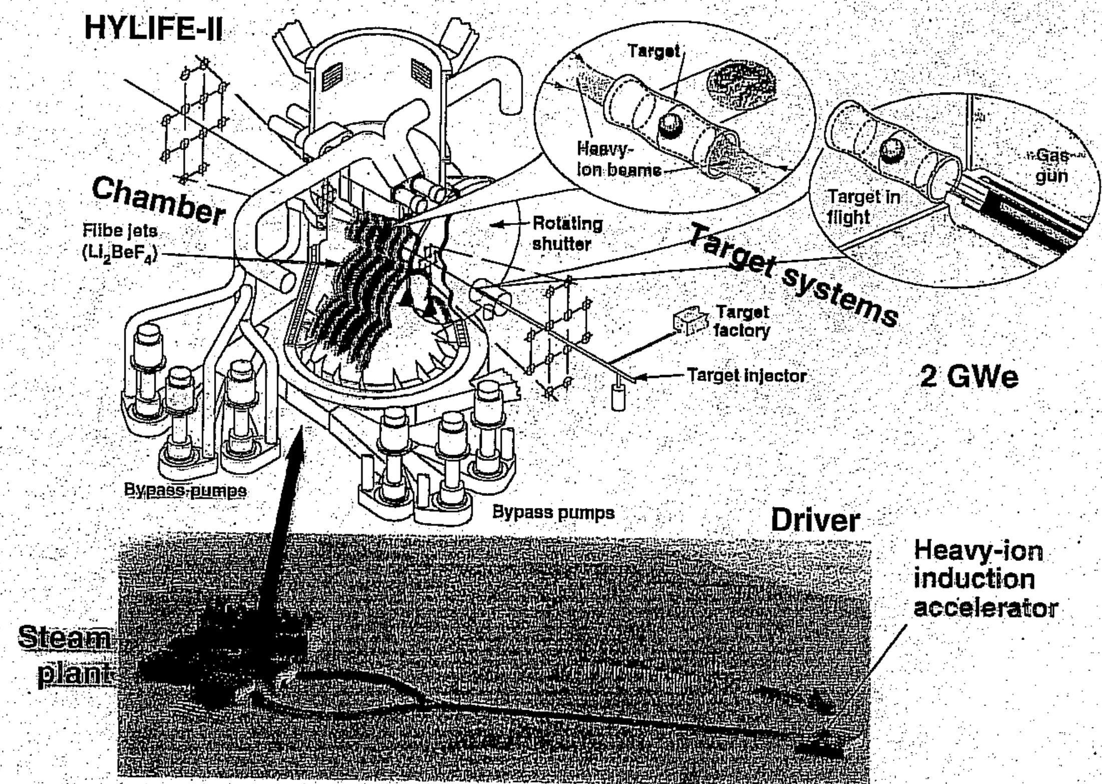

Liquid-jet protected fusion chambers for long lifetime, low cost, and low environmental impact

A number of final focus options are being considered for HIF applications

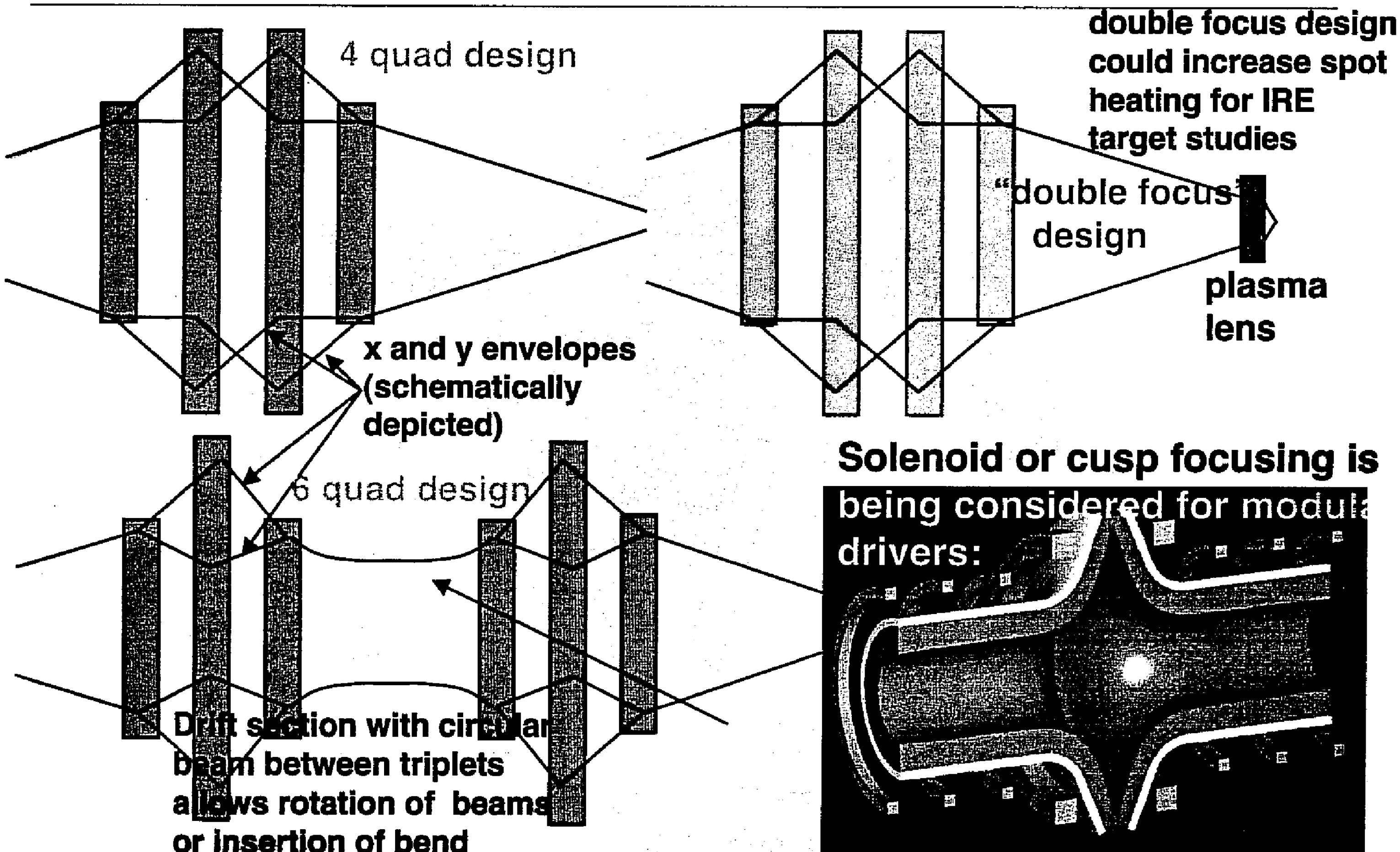

Estimating Spot Size

$$r_x'' + \frac{(\gamma_b\beta_b)'}{\gamma_b\beta_b} r_x + k_x r_x - \frac{2Q}{r_x+r_y} - \frac{\varepsilon_x^2}{r_x^3} = 0$$

$$r_y'' + \frac{(\gamma_b\beta_b)'}{\gamma_b\beta_b} r_y + k_y r_y - \frac{2Q}{r_x+r_y} - \frac{\varepsilon_y^2}{r_y^3} = 0$$

In chamber: No external focusing, no acceleration and beam is often circular (by design)

$$\Rightarrow \quad k_x = k_y = (\gamma_b\beta_b)' = 0 \quad \& \quad r_x = r_y = r_b$$

$\Rightarrow$ Envelope equation is:

$$r_b'' = \frac{Q}{r_b} + \frac{\epsilon^2}{r_b^3}$$

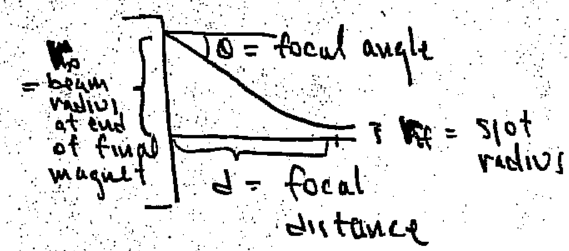

Multiplying by r_b' & integrating $\Rightarrow$

$$\frac{r_{bf}'^2}{2} - \frac{r_{bo}'^2}{2} = Q \ln\frac{r_{bf}}{r_{bo}} + \frac{\epsilon^2}{2r_{bo}^2} - \frac{\epsilon^2}{2r_{bf}^2}$$

Now $\quad r_{bo}' \cong \theta \qquad r_{bf} = \text{spot radius} \qquad r_{bf} << r_{bo}$

$\qquad r_{bf}' = 0 \qquad r_{bo} \cong d\theta$

$$\Rightarrow \boxed{\theta^2 \cong 2Q \ln\left(\frac{\theta d}{r_{bf}}\right) + \frac{\epsilon^2}{r_{bf}^2}}$$

For emittance dominated spot: $\quad r_{bf} = \dfrac{\epsilon}{\theta}$

"CHROMATIC ABERRATIONS" TEND TO BROADEN SPOT

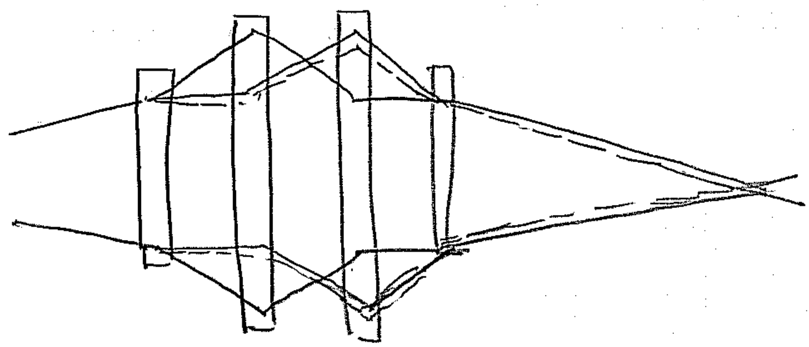

SINCE QUADRUPOLE MAGNET FOCUSING $\propto \frac{1}{V_z}$

(i.e. $x'' = \frac{qB'}{\gamma m v_z} x$) A SPREAD IN LONGITUDINAL VELOCITY GIVES RISE TO A BROADENING OF FINAL SPOT.

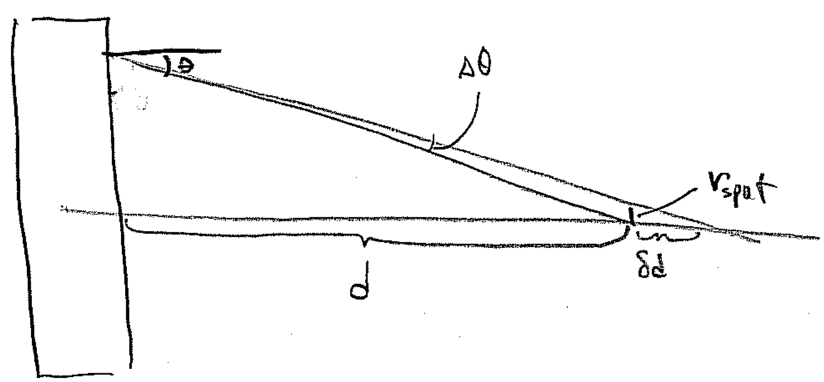

$$r_{spot} = \theta\, \delta d$$
$$= \theta \frac{dd}{d\theta} \frac{d\theta}{dp} \delta_p$$
$$= \alpha\, \theta\, d \left(\frac{\delta p}{p}\right)$$

α = some constant depending on focal system

HEURISTICALLY THE CONTRIBUTION FROM CHROMATIC ABERRATIONS CAN BE WRITTEN

$$r^2_{chrom} = \alpha^2 d^2 \left(\frac{\delta\gamma}{\gamma}\right)^2 \theta^2$$

where α depends on system, typically 4-8

$$r^2_{spot} = r^2_{bf} + r^2_{chrom}$$

DETAILED SIMULATIONS OR MOMENT CODE RESULTS REQUIRED TO FIX α.

How can we estimate the coefficient for chromatic aberrations?

We constructed moment models to study chromatic effects (through 2nd order) in final focus system

$$\frac{dp_x}{dt} = q(E_x + v_z B_y - v_y B_z)$$

Expand through 2nd order in x', y', $k_{\beta 0}x$, $k_{\beta 0}y$, $\delta p/p$

$$x'' + \left(\frac{1}{\gamma v_{z0}}\frac{d}{dz}(\gamma v_z)\right)x' \cong \frac{qB'}{\gamma m v_{z0}} x\left(1-\frac{\delta p}{p}\right) + \frac{q\lambda}{4\pi\varepsilon_0 m v_{z0}^2}\frac{(x-\bar{x})(1-\frac{2\delta p}{p})}{(\Delta x^2 + [\Delta x^2 \Delta y^2]^{1/2})}$$

The equation of motions can be written (where $\delta = \delta p/p$) **:**

$$\boxed{x'' \cong K_{xx}x + K_{xx1}x\delta \qquad y'' \cong K_{yy}y + K_{yy1}y\delta}$$

Here:

$$K_{xx} = \frac{B'}{[B\rho]_0} + \frac{Q}{2(\Delta x^2 + [\Delta x^2 \Delta y^2]^{1/2})} \qquad K_{yy} = \frac{-B'}{[B\rho]_0} + \frac{Q}{2(\Delta y^2 + [\Delta x^2 \Delta y^2]^{1/2})}$$

$$K_{xx1} = -\left[\frac{B'}{[B\rho]_0} + \frac{2Q}{2(\Delta x^2 + [\Delta x^2 \Delta y^2]^{1/2})}\right] \qquad K_{yy1} = -\left[\frac{-B'}{[B\rho]_0} + \frac{2Q}{2(\Delta y^2 + [\Delta x^2 \Delta y^2]^{1/2})}\right]$$

$B' =$ **quadrupole gradient;** $[B\rho] =$ **Ion rigidity** $= p/q$; $Q =$ **perveance** $= \dfrac{q\lambda}{2\pi\varepsilon_0 \gamma_0^3 m v_{z0}^2}$

We take averages of 2nd, 3rd,… order quantities, forming infinite set of 1st order ode's

$$\frac{d}{ds}\left\langle x^2 \right\rangle = 2\left\langle xx' \right\rangle$$

$$\frac{d}{ds}\left\langle xx' \right\rangle = \left\langle x'^2 \right\rangle + \left\langle xx'' \right\rangle$$

$$= \left\langle x'^2 \right\rangle + K_{xx}\left\langle x^2 \right\rangle + \underline{K_{xx1}\left\langle x^2\delta \right\rangle}$$

$$\frac{d}{ds}\left\langle x'^2 \right\rangle = 2\left\langle x'x'' \right\rangle$$

$$= 2K_{xx}\left\langle xx' \right\rangle + \underline{2K_{xx1}\left\langle xx'\delta \right\rangle}$$

$$\frac{d}{ds}\left\langle x^2\delta \right\rangle = 2\left\langle xx'\delta \right\rangle$$

$$\frac{d}{ds}\left\langle xx'\delta \right\rangle = \left\langle x'^2\delta \right\rangle + \left\langle xx''\delta \right\rangle$$

$$= \left\langle x'^2\delta \right\rangle + K_{xx}\left\langle x^2\delta \right\rangle + \underline{K_{xx1}\left\langle x^2\delta^2 \right\rangle}$$

$$\frac{d}{ds}\left\langle x'^2\delta \right\rangle = 2\left\langle x'x''\delta \right\rangle$$

$$= 2K_{xx}\left\langle xx'\delta \right\rangle + \underline{2K_{xx1}\left\langle xx'\delta^2 \right\rangle}$$

…

$$\frac{d}{ds}\left\langle x^2\delta^n \right\rangle = 2\left\langle xx'\delta^n \right\rangle$$

$$\frac{d}{ds}\left\langle xx'\delta^n \right\rangle = \left\langle x'^2\delta^n \right\rangle + \left\langle xx''\delta^n \right\rangle$$

$$= \left\langle x'^2\delta^n \right\rangle + K_{xx}\left\langle x^2\delta^n \right\rangle + \underline{K_{xx1}\left\langle x^2\delta^{n+1} \right\rangle}$$

$$\frac{d}{ds}\left\langle x'^2\delta^n \right\rangle = 2\left\langle x'x''\delta^n \right\rangle$$

$$= 2K_{xx}\left\langle xx'\delta^n \right\rangle + \underline{2K_{xx1}\left\langle xx'\delta^{n+1} \right\rangle}$$

=> term higher order by one

Infinite set of equations can be truncated, but are reliable over only finite distances

Two equivalent methods of truncation have been employed:

1. $\langle x^2\delta^2\rangle \approx \langle x^2\rangle\langle\delta^2\rangle$ **and** $\langle xx'\delta^2\rangle \approx \langle xx'\rangle\langle\delta^2\rangle$ **; or**

2. Noticing that $\frac{1}{1+\delta} = 1-\delta+\delta^2+\ldots$ **and** $\frac{1}{1-\delta} = 1+\delta+\delta^2+\ldots$ **thus,**

$\frac{1}{1-\delta} - \frac{1}{1+\delta} = 2\delta + 2\delta^3 + \ldots$ **also** $\frac{\delta}{1+\delta} = 1 - \frac{1}{1+\delta}$

so that we may, to good approximation, write

$$\frac{d}{ds}\langle x^2\rangle = 2\langle xx'\rangle \qquad \frac{d}{ds}\langle xx'\rangle = \langle x'^2\rangle + K_{xx}\langle x^2\rangle + \frac{K_{xx1}}{2}\left[\left\langle\frac{x^2}{1-\delta}\right\rangle - \left\langle\frac{x^2}{1+\delta}\right\rangle\right] + O\left(x^2\delta^3\right)$$

$$\frac{d}{ds}\langle x'^2\rangle = 2K_{xx}\langle xx'\rangle + K_{xx1}\left[\left\langle\frac{xx'}{1-\delta}\right\rangle - \left\langle\frac{xx'}{1+\delta}\right\rangle\right] + O(xx'\delta^3)$$

$$\frac{d}{ds}\left\langle\frac{xx'}{1+\delta}\right\rangle = \left\langle\frac{x'^2}{1+\delta}\right\rangle + K_{xx}\left\langle\frac{x^2}{1+\delta}\right\rangle - K_{xx1}\left\langle\frac{x^2}{1+\delta}\right\rangle + K_{xx1}\langle x^2\rangle \qquad \frac{d}{ds}\left\langle\frac{x^2}{1+\delta}\right\rangle = 2\left\langle\frac{xx'}{1+\delta}\right\rangle$$

$$\frac{d}{ds}\left\langle\frac{x'^2}{1+\delta}\right\rangle = 2K_{xx}\left\langle\frac{xx'}{1+\delta}\right\rangle + 2K_{xx1}\langle xx'\rangle - 2K_{xx1}\left\langle\frac{xx'}{1+\delta}\right\rangle$$

Truncated set of equations forms closed set.

both methods give nearly identical results for $\langle\delta^2\rangle$ **in the regime of interest; similar equations for** $\langle x^2/(1-\delta)\rangle$, $\langle xx'/(1-\delta)\rangle$, $\langle x'^2/(1-\delta)\rangle$, **and the same set for** y**; 18 equations total.**

Comparison of moment equations with Particle-in-Cell (WARP[1]) simulations (1% velocity spread)

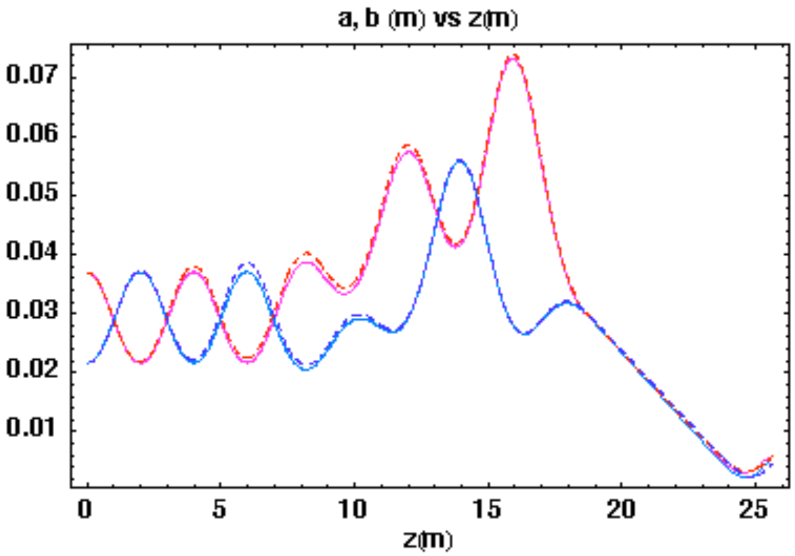

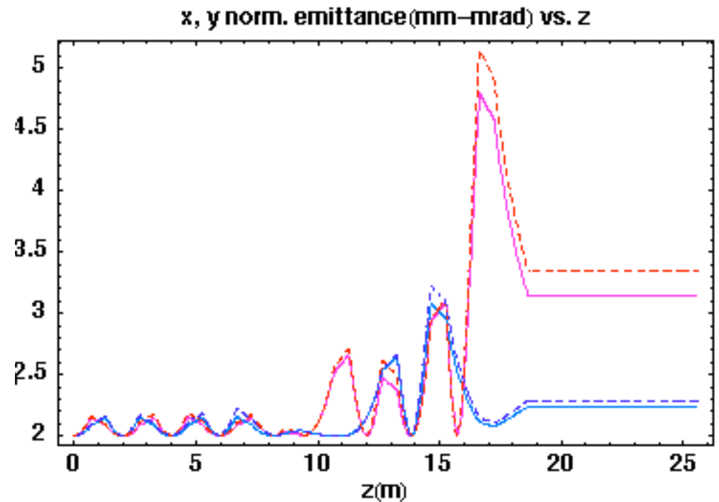

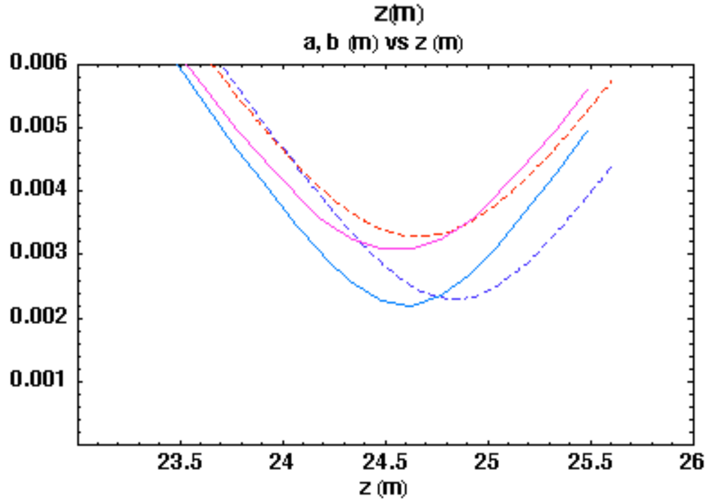

Particle simulations:
Dashed, red (x) and blue (y)
Initial distribution: KV

Moment calcluations:
Solid, magenta (x), and aqua (y)

Result: $$\varepsilon_{xc} \cong \alpha_{cx} d \left(\frac{\delta p}{p} \right) \theta_x^2$$

α_{cx}= 4 -12 depending on geometry and initial $\langle x\delta p \rangle$

Comparison of moment equations with PIC simulations (WARP) -- no velocity spread

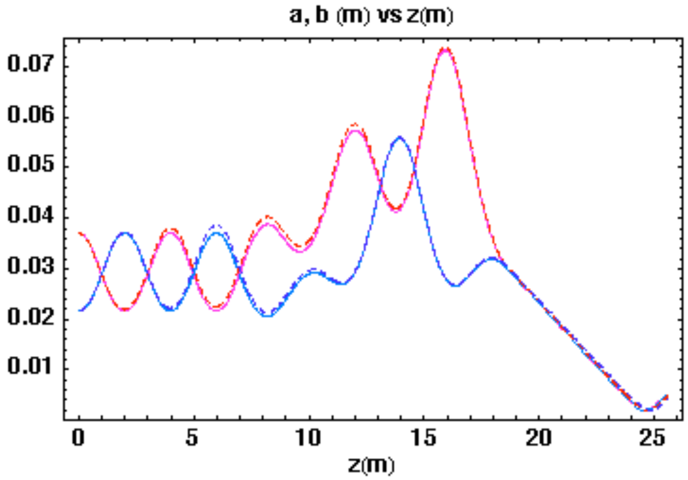

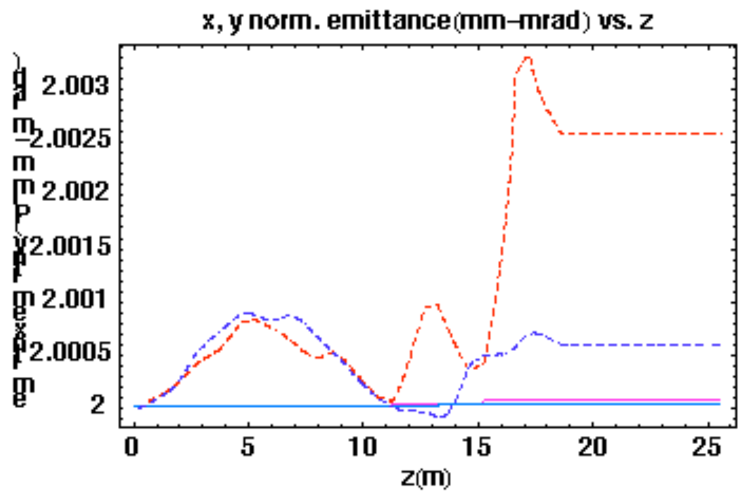

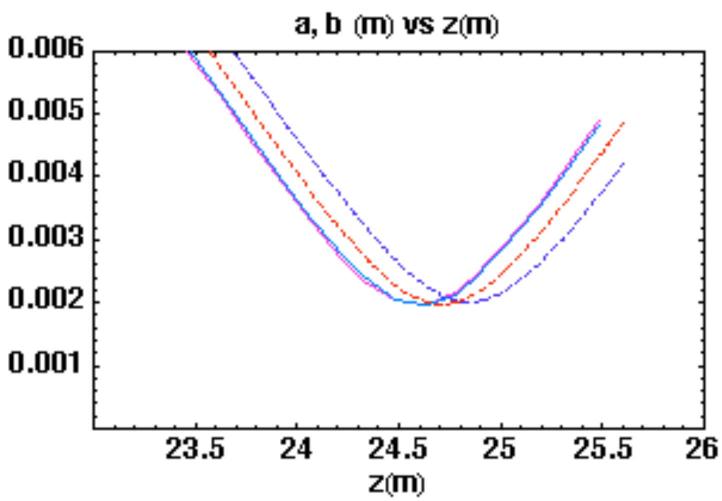

Particle simulations: Dashed, red (x) and blue (y)
Initial distribution: KV
Moment calcluations: Solid, magenta (x), and aqua (y)

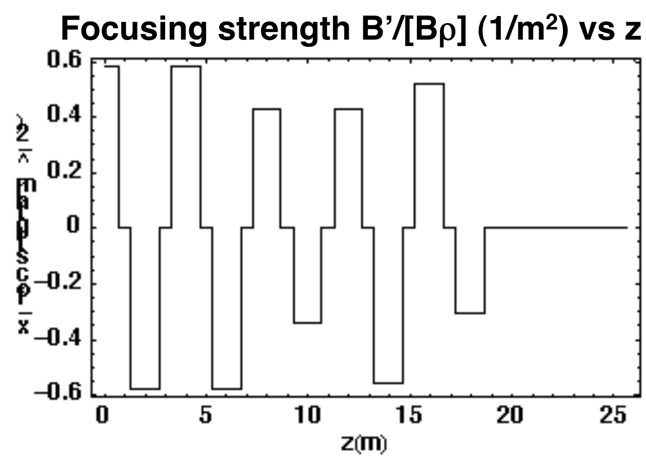

The HIFS VNL has a plan for using present and future accelerators for WDM and HIF experiments

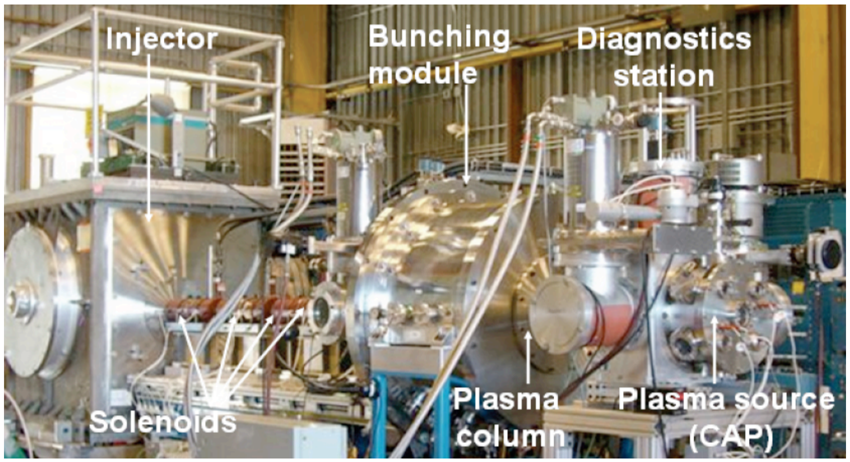

Recent Experiment

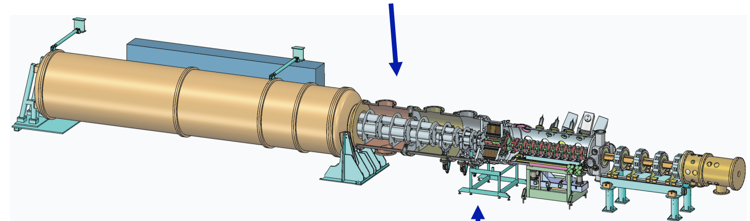

← Current Experiment

NDCX I

0.4 MeV, 0.003 μC

HCX

1.7 MeV, ~0.025 μC

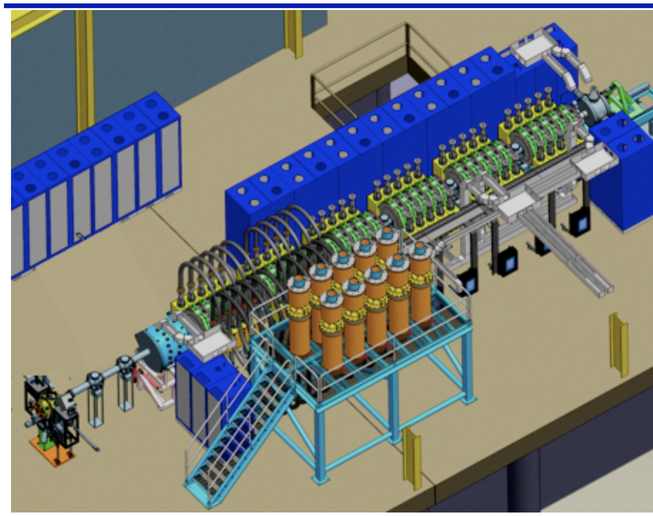

NDCX II
1.2 - 3 MeV, 0.03 μC
Under construction:
Completion date: 2012

IB-HEDPX
5 - 15 year goal
20 - 40 MeV, 0.3 - 1.0 μC
WDM User facility

← Future Experiments

10 kJ Machine for HIF
10 - 20 year goal
Target implosion physics

HIF/WDM beam science: neutralized focusing and neutralized drift compression are being tested now for use in WDM and HIF applications

Both techniques minimize the effects of space charge on transverse and longitudinal compression

Transverse compression: vapor from liquid walls in HIF chamber would strip beam, so neutralization required to focus beam in liquid walled chamber. Recent VNL experiments, eg. scaled final focus experiment, (MacLaren et al 2002), NTX (Roy et al 2004), and current NDCX-1 have demonstrated benefits of neutralization by plasmas

Longitudinal compression: WDM experiments require very short, intense pulses (<~ 1 ns) (shorter durations than required by HIF). Neutralization allows what would be very high perveance beams in absence of neutralization (~ 10^{-2}). Modular HIF concept also pushes limits of high perveance beams (since ions have lower accumulated voltage to minimize accelerator length).

Artist's conception of HIF Power Plant on a few km^2 site